

Controlling Atomic Layer Deposition of TiO₂ in Aerogels through Surface Functionalization

Sutapa Ghosal,^{*,†} Theodore F. Baumann,[†] Jeffrey S. King,[‡] Sergei O. Kucheyev,[†]
Yinmin Wang,[†] Marcus A. Worsley,[†] Juergen Biener,[†] Stacey F. Bent,[‡] and
Alex V. Hamza[†]

Nanoscale Synthesis and Characterization Laboratory, Lawrence Livermore National Laboratory, 7000
East Avenue, Livermore, California 94550, and Department of Chemical Engineering, Stanford University,
381 North South Mall, Stanford, California 94305

Received March 5, 2009

This report demonstrates a chemical functionalization method for controlling TiO₂ ALD in low-density nanoporous materials, i.e., aerogels. Functionalization of silica aerogel with trimethylsilane is shown to inhibit TiO₂ growth on the aerogel via ALD. A proposed mechanism for the deactivation effect is the blocking of surface functional groups, such as hydroxyl (OH) moieties, which serve as chemisorption sites for the ALD precursors and hence are essential for nucleating the deposition process. Subsequent modification of the aerogel functionalization through the selective removal of hydrocarbon groups via heat or plasma treatment reactivates the aerogel towards deposition, thereby resulting in TiO₂ growth. The results presented here demonstrate the use of ALD as a selective tool for creating novel nanoporous materials.

Introduction

Nanoporous materials present significant technological advantage for a wide range of applications, including catalysis, energy storage and conversion, and nanoelectronics, to name just a few.^{1–4} Hence, there is considerable interest in developing synthetic pathways for the fabrication of nanoporous materials with tailored properties. Aerogels (AGs) are unique low-density, open-cell porous materials consisting of submicrometer pores and ligaments that can be used as a robust material platform for designing novel nanoporous materials. In recent years, a synthetic approach based on ALD on AG templates has emerged as a promising method for the directed growth of nanoporous materials.^{5–11,18} This approach has been used successfully to prepare millimeter-sized high aspect ratio aerogels coated uniformly with zinc oxide (ZnO), tungsten (W), and alumina (Al₂O₃).^{10,11}

The ALD process utilizes two sequential, self-limiting surface reactions resulting in a layer-by-layer growth mode. The self-limiting nature of the surface reactions makes ALD

a particularly suitable technique for uniform deposition onto high aspect ratio porous substrates. Additionally, chemical specificity of the surface reactions in ALD enables one to control the deposition process through selective functionalization of the substrate surface. In fact, the functionalization of planar substrates such as silicon wafers with organosilane groups (R_nSiX_{4–n} (n = 1–3)) has been shown to deactivate the substrate toward ZrO₂, HfO₂, ZnO, and TiO₂ ALD processes.^{12–16} A possible mechanism for the deactivation effect is the blocking of surface functional groups, such as hydroxyl (OH) moieties, which serve as chemisorption sites for the ALD precursors and hence are essential for nucleating the deposition process. Henceforth, we shall refer to these surface functional groups as nucleation sites for the ALD process.

All previous reports on the use of organosilane functionalization of surfaces to control ALD have focused exclusively on two-dimensional planar substrates such as silicon wafers.^{12–16} However, the use of organosilane functionalization presents an attractive approach for controlling ALD in three-dimensional (3D) high aspect ratio nanoporous substrates such as AGs. Selective deposition onto a substrate can be achieved by controlling the deactivation and subsequent reactivation of the substrate toward deposition in a systematic manner. In this communication, we demonstrate that the reactivity of SiO₂ AGs toward TiO₂ ALD^{17,18} can be switched off and on by controlling the functionalization

[†] Lawrence Livermore National Laboratory.

[‡] Stanford University.

- (1) Weissmüller, J.; Viswanath, R. N.; Kramer, D.; Zimmer, P.; Würschum, R.; Gleiter, H. *Science* **2003**, *300*, 312.
- (2) Chan, S.; Kwon, S.; Koo, T. W.; Lee, L. P.; Berlin, A. A. *Adv. Mater.* **2003**, *15*, 1595.
- (3) Kramer, D.; Viswanath, R. N.; Weissmüller, J. *Nano Lett.* **2004**, *4*, 793.
- (4) He, X.; Antonelli, D. *Angew. Chem., Int. Ed.* **2002**, *41*, 214.
- (5) Zhao, X. S.; Su, F.; Yan, Q.; Guo, W.; Bao, X. Y.; Lv, L.; Zhou, Z. *J. Mater. Chem.* **2006**, *16*, 637.
- (6) Stein, A. *Adv. Mater.* **2003**, *15*, 763.
- (7) Schüth, F. *Angew. Chem., Int. Ed.* **2003**, *42*, 3604.
- (8) Davis, M. *Nature (London)* **2002**, *417*, 813.
- (9) Huczko, A. *Appl. Phys. A: Mater. Sci. Process.* **2000**, *70*, 365.
- (10) Kucheyev, S. O.; Biener, J.; Wang, Y. M.; Baumann, T. F.; Wu, K. J.; Van Buuren, T.; Hamza, A. V.; Satcher, J. H., Jr.; Elam, J. W.; Pellin, M. J. *Appl. Phys. Lett.* **2005**, *86* (8), 1.
- (11) Baumann, T. F.; Biener, J.; Wang, Y. M.; Kucheyev, S. O.; Nelson, A. J.; Satcher, J. H.; Elam, J. W.; Pellin, M. J.; Hamza, A. V. *Chem. Mater.* **2006**, *18* (26), 6106.

- (12) Chen, R.; Kim, H.; McIntyre, P. C.; Bent, S. F. *Appl. Phys. Lett.* **2004**, *84*, 4017.
- (13) Yan, M.; Koide, Y.; Babcock, J. R.; Markworth, P. R.; Belot, J. A.; Marks, T. J.; Chang, R. P. H. *Appl. Phys. Lett.* **2001**, *79*, 1709.
- (14) Park, M. H.; Jang, Y. J.; Sung-Suh, H. M.; Sung, M. M. *Langmuir* **2004**, *20*, 2257.
- (15) Chen, R.; Kim, H.; McIntyre, P. C.; Bent, S. F. *Chem. Mater.* **2005**, *17*, 536.
- (16) Chen, R.; Kim, H.; McIntyre, P. C.; Porter, D. W.; Bent, S. F. *Appl. Phys. Lett.* **2005**, *86*, 191910.
- (17) Ritala, M.; Leskelä, M.; Nykänen, E.; Soininen, P.; Niinistö, L. *Thin Solid Films* **1993**, *225* (1–2), 288.

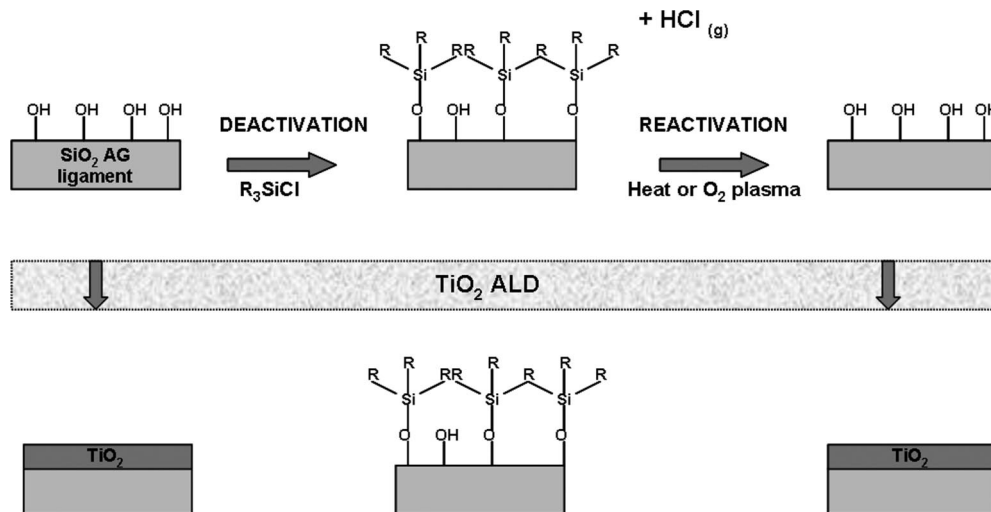


Figure 1. Schematic illustration of selective TiO_2 ALD in silica aerogel through functionalization of aerogel ligaments, $\text{R} = \text{CH}_3$.

of the AG ligament network. Specifically, we demonstrate (i) the passivation of SiO_2 AGs by the capping of nucleation sites with trimethylsilyl (TMS) groups and (ii) subsequent reactivation of the AG through selective removal of the methyl capping groups by heat or oxygen plasma treatment. TiO_2 was chosen as the growth material in our study because of its significance as a photocatalyst with promising energy and environmental applications.^{18–21} The synthetic approach presented here can potentially be extended in the future to create 3D patterned nanoporous solids, for instance, through spatial localization of the reactivation process.

Experimental Section

Amorphous SiO_2 AGs with monolith densities of $\sim 120 \text{ mg/cm}^3$ were used in this study. The aerogel templates, with pores and ligaments of tens of nanometers length scale, were synthesized as described in detail elsewhere.²² TMS functionalization of SiO_2 AG was achieved by exposure of the wet SiO_2 gels to chlorotrimethylsilane (CTMS) prior to supercritical extraction. Specifically, the wet SiO_2 gels were subjected to consecutive solvent exchanges in ethanol (48 h) and hexane (24 h), followed by exposure to CTMS solution (50 wt % in hexane) for 72 h to promote functionalization. The functionalized wet gels were then subjected to further solvent exchanges in hexane (24 h) and ethanol (24 h) before being dried by supercritical carbon dioxide to form the aerogel.

TiO_2 ALD on centimeter-sized AG monoliths was performed through alternating exposures to titanium tetrachloride (TiCl_4) and water (H_2O) in an ALD reactor at a sample stage temperature of 100°C and a reactor wall temperature of 125°C . Note that TiCl_4 is a very reactive precursor and thus well suited to test the degree of surface passivation. Growth of TiO_2 on the planar SiO_2 substrate via ALD under similar conditions has been demonstrated previously.²³ To increase heat transfer from the sample stage to the AG monoliths, hot wall conditions were replicated by placing the monoliths inside a machined aluminum container with a perforated lid. The

container was then placed inside the reactor directly on the heated stage. The SiO_2 AG templates with and without CTMS functionalization were exposed to five ALD cycles simultaneously. Each cycle consisted of a 30 s TiCl_4 pulse followed by a 120 s dry nitrogen (N_2) purge and a 30 s H_2O vapor pulse followed again by a 120 s N_2 purge. For planar SiO_2 substrates, similar deposition conditions resulted in a TiO_2 growth rate of $\sim 0.5 \text{ \AA/cycle}$. Deposition of TiO_2 onto the AGs was examined by Rutherford backscattering spectrometry (RBS) with 2 MeV $^4\text{He}^+$ ions backscattered to 164° and by synchrotron based X-ray fluorescence (XRF) measurements at the Advanced Photon Source. In RBS measurements depth uniformity of the deposited Ti concentration was determined based on RUMP code²⁴ simulations, as described in detail elsewhere.²⁵ In RUMP simulations, the composition of the AG ligaments following TiO_2 deposition was defined as $\text{SiO}_{2(1+x)}\text{Ti}_x$. Surface area of the AGs prior to deposition was measured using the Brunauer–Emmett–Teller (BET) method. Morphology of the resulting $\text{TiO}_2/\text{SiO}_2$ nanocomposite was characterized in a Philips FEG-300 transmission electron microscope (TEM).

Results and Discussion

A schematic outline of our approach to deactivation and subsequent reactivation of the SiO_2 AG template toward TiO_2 ALD is shown in Figure 1. Chloro-organosilane deactivating agents are known to react with surface OH groups, leaving alkylsilyl groups bonded to the surface through covalent Si–O bonds.¹⁶ Therefore, deactivation of the SiO_2 AG template by TMS is expected to occur by the following two mechanisms: (1) silylation of the reactive surface OH groups and (2) steric blocking of the SiO_2 surface by TMS groups since TiO_2 nucleation is believed to be possible at the Si–O–Si sites as well as the surface hydroxyl groups.^{15,17}

Functionalization of the AG network with TMS drastically reduces TiO_2 deposition on the AG, as evident from the RBS results shown in Figure 2. The RBS measurements give Ti atomic concentrations of 1.9% and 9.5% for TMS functionalized and nonfunctionalized AGs, respectively. This corresponds to a 5 times lower TiO_2 deposition on the TMS functionalized AG. In both cases, TiO_2 deposition is uniform up to a depth of $\sim 20 \mu\text{m}$ (the maximum depth probed in

(18) Hamann, T. W.; Martinson, A. B. F.; Elam, J. W.; Pellin, M. K.; Hupp, J. T. *J. Phys. Chem. C* **2008**, *112*, 10303.

(19) O'Regan, B.; Grätzel, M. *Nature (London)* **1991**, *353*, 737.

(20) Grätzel, M. *Nature (London)* **2001**, *414*, 338.

(21) Barbé, C. J.; et al. *J. Am. Ceram. Soc.* **1997**, *80*, 3157.

(22) Hrubesh, L. W.; Tillotson, T. M. J.; Poco, F. In *Chemical Processing of Advanced Materials*; Hench, L. L., West, J. K., Eds.; Wiley: New York, 1992; p 19.

(23) Aarik, J.; Aidla, A.; Mändar, H.; Uustare, T. *Appl. Surf. Sci.* **2001**, *172*, 142.

(24) Doolittle, L. R. *Nucl. Instrum. Methods* **1985**, *B9*, 344.

(25) Kucheyev, S. O.; Biener, J.; Baumann, T. F.; Wang, Y. M.; Hamza, A. V.; Li, Z.; Lee, D. K.; Gordon, R. G. *Langmuir* **2008**, *24* (3), 943.

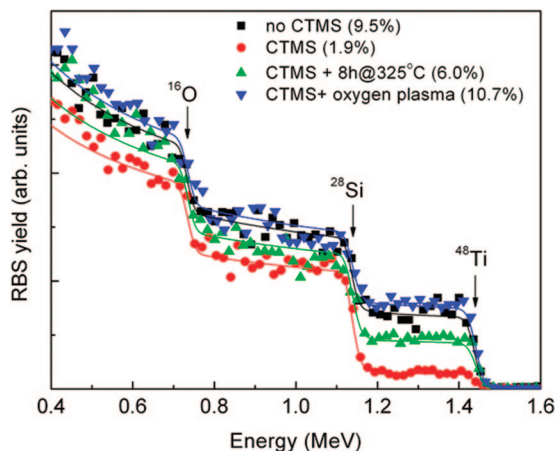


Figure 2. RBS spectra from TiO₂-coated silica AGs (~120 mg/cm³). Positions of the surface peaks of O, Si, and Ti are denoted by arrows. For clarity, only every fifth experimental point is depicted. Solid lines are results of RUMP simulations. ALD parameters are the same for all four AGs. The legend gives values of Ti atomic percent obtained by fitting RUMP simulation curves to experimental spectra.

Table 1. Density and Brunauer–Emmett–Teller Surface Area of Amorphous Silica Aerogel Substrates Used in This Study

aerogel	density (mg/cm ³)	specific surface area (m ² /g)
SiO ₂	100	308
SiO ₂ /CTMS	120	631

our RBS analysis of the 120 mg/cm³ AG). Deactivation of the AG by TMS functionalization has also been confirmed by our XRF measurements wherein the Ti fluorescence signal, following TiO₂ ALD, from the functionalized AG is minimal compared to the nonfunctionalized AG. Similar TiO₂ deposition behavior was also observed in the case of lower density, 20 mg/cm³, AG templates under identical deposition conditions. We expect that our surface passivation would be even more effective for less reactive ALD precursors such as the [Ti(OPrⁱ)₄] precursor used by Park et al. in their work involving a planar silica substrate.¹⁴ Further optimization of the deactivation effect may also be possible through experimentation with different functional groups as the deactivating agent.

Specific surface areas of the SiO₂ AG monoliths used in our study are given in Table 1. Interestingly, the TMS functionalized SiO₂ AG has a larger surface area relative to the nonfunctionalized AG. Functionalization of the SiO₂ AG with hydrophobic TMS groups is known to inhibit unwanted condensation reactions within the wet gel.²⁶ This in turn may help to minimize any associated loss in AG surface area due to cross-linking of the AG ligaments during the wet gel stage. In our experiments there was a lag period between the synthesis of the wet gel and the subsequent supercritical extraction of the AG. In the case of the nonfunctionalized wet gel, additional condensation reactions during the lag period most likely account for its lower surface area compared to the functionalized AG. Measured surface area of the functionalized AG in our experiments is in good agreement with the surface area reported by Schwertfeger et al. for 160 mg/cm³ TMS functionalized SiO₂ AG.²⁷

Additionally, it is also possible that TMS functionalization leads to roughening of the AG ligament surface with a resultant increase in the overall AG surface area. It is important to note that, independent of its origin, the increased surface area of the functionalized aerogels results in an underestimation of the effectiveness of the TMS passivation. Accounting for the roughly three times higher surface area of the functionalized aerogels, the presence of trimethylsilyl capping groups suppresses the deposition of TiO₂ by a factor of 15 rather than 5. This highlights the significance of surface nucleation sites in the ALD growth process and the role played by TMS in the deactivation of these nucleation sites.

Figure 3 shows bright-field TEM images of the SiO₂ AGs before and after TiO₂ ALD and of the TMS functionalized AG after ALD. The ligament width for both the functionalized and nonfunctionalized AGs before ALD is ~8–10 nm (Figure 3A). The deposited TiO₂ is not readily distinguishable from the underlying SiO₂ substrate since the TEM images of the untreated and TiO₂-coated AGs do not show any detectable differences in their ligament size. Therefore, based on the observation that TiO₂ deposition does not lead to any obvious change in the AG ligament morphology, the overall AG surface area following deposition is not expected to change under these conditions. Area-selective TEM-EDX analysis of the AGs following deposition further confirms the significant difference in TiO₂ content between the functionalized and the nonfunctionalized AGs (Figure 3D,E). For the nonfunctionalized AG the Ti/Si ratio was found to be nearly independent of the size of the analyzed area ranging from larger sample fragments down to the single ligament level. In comparison, hardly any Ti signal was detected from the ligaments of the functionalized AG. These results are consistent with our RBS and XRF data, suggesting that TiO₂ growth requires the presence of chemisorption sites for the ALD precursors.

Next, we evaluated different sample treatments in terms of their effectiveness in reactivating the TMS functionalized SiO₂ AGs toward TiO₂ ALD. The objective was to selectively remove methyl (CH₃) capping groups with minimal perturbation of the AG architecture. We exposed the TMS-capped AG to one of the following two reactivation treatments: (1) heating in a tube furnace at 325 °C in air for 8 h or (2) oxygen plasma exposure in a Branson/IPC Asher (300 W, 80 sccm, 44 mTorr) for 3 min. Following the reactivation treatment AG samples were exposed to five cycles of TiO₂ ALD. RBS measurements gave Ti atomic concentrations of 6.0% and 10.7% for heat and plasma treated AGs, respectively (Figure 2). By comparison Ti atomic concentrations for the nonfunctionalized and functionalized AGs without the reactivation treatment were 9.5% and 1.9%, respectively (Figure 2). The Ti atomic concentration for the plasma treated AG is ~2 times greater than the heat treated sample. Therefore, oxygen plasma exposure is the more effective of the two treatments in restoring reactivity of the TMS functionalized AG toward TiO₂ ALD. Neither plasma nor heat treatment resulted in the loss of AG surface area. Hence the reactivation treatments appear to have minimal impact on the overall AG architecture.

(26) Smith, D. M.; Stein, D.; Anderson, J. M.; Ackerman, W. J. *Non-Cryst. Solids* **1995**, 186, 104.

(27) Schwertfeger, F.; Frank, D.; Schmidt, M. J. *Non-Cryst. Solids* **1998**, 225, 24.

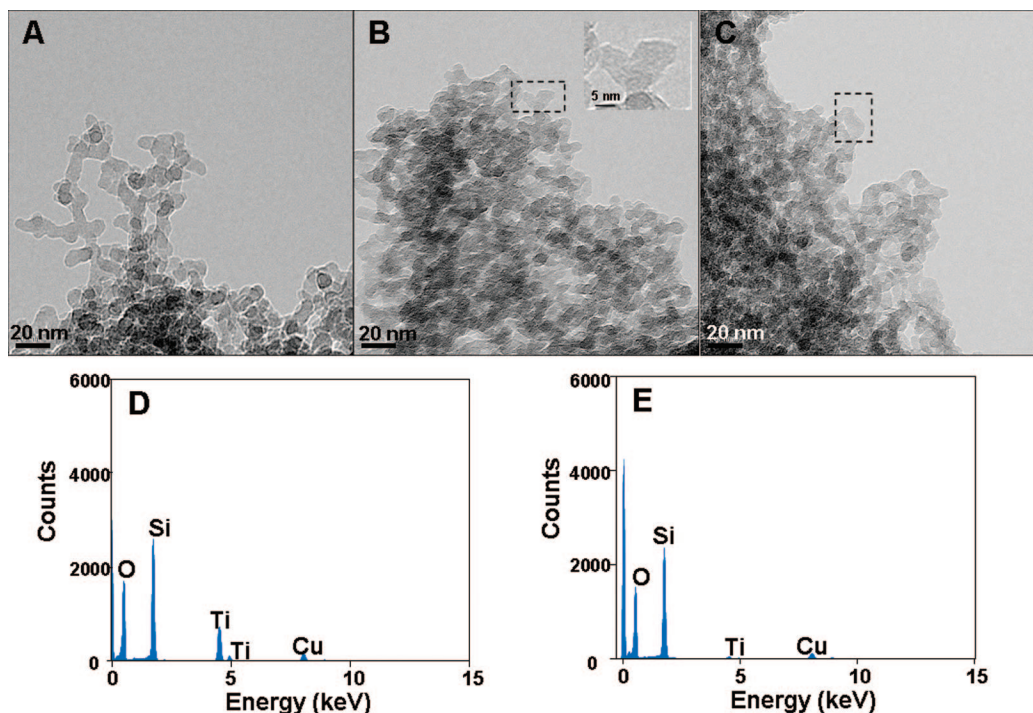


Figure 3. TEM images of silica AG (A) before ALD, (B) following five cycles of TiO_2 ALD, and (C) CTMS functionalized silica AG following five cycles of TiO_2 ALD. (D and E) Corresponding EDS spectra obtained from a single ligament (dotted box) in (B) and (C), respectively, using an electron beam size of 1.2 nm. The inset in (B) is a close-up image of the region highlighted by the dotted box. The copper (Cu) signal in the EDS spectra is from the Cu TEM grids used in the measurements.

Both reactivation approaches described above rely on the oxidative degradation of the organic capping groups.²⁸ For example, the use of oxygen plasma to remove hydrocarbon resists is a well established technique in microelectronic device fabrication.²⁹ The reactivation process restores the original surface chemistry as it leaves the substrate functionalized with OH groups. However, the authors want to point out that the reactivation treatment does not remove the intact trimethylsilyl capping group but leaves an additional Si atom per capping group behind. Compared to thermal oxidation, the availability of reactive species (i.e., atomic oxygen) in the plasma seems to enhance the degradation process.²⁸ Surprisingly, plasma treatment is successful in reactivating the AG up to a depth of $\sim 20\ \mu\text{m}$, the maximum depth probed in our RBS analysis for the $120\ \text{mg}/\text{cm}^3$ AG. This observation suggests that the plasma induced reactivation mechanism is not limited to line of sight etching by plasma generated reactive species. It is possible that atomic oxygen has a low sticking and recombination probability in SiO_2 AG, thus allowing for its penetration into the pores of the AG and the resultant reactivation of subsurface active sites. It is also plausible that these reactive species are generated in situ within the pores of the AG by penetration of the plasma inside the nonconductive and nanoporous network, thereby promoting bulk reactivation. However, further studies need to be done to verify this hypothesis.

Conclusion

In summary, we have shown that functionalization of a SiO_2 AG template with organosilane groups inhibits TiO_2

ALD on the high aspect ratio nanoporous structure. This approach can possibly be applied to other ALD processes as well which require the presence of surface OH as nucleation sites. Additionally, we have demonstrated reactivation of the functionalized AG template for TiO_2 deposition through direct removal of the hydrocarbon capping groups. The synthetic approach presented here can potentially be extended to fabricate 3D structured nanoporous materials by using direct laser writing methods to locally reactivate a passivated AG template.^{30,31} For instance, photosensitive capping groups can be used to facilitate localized photoinduced reactivation of the AG. It may also be possible to take advantage of the low thermal conductivity of AGs to promote localized thermally induced reactivation by using laser light to locally heat the AG template. Dulcey et al. have already demonstrated the feasibility of the first approach in the case of a functionalized planar silica substrate.³² The ability to control the ALD nucleation process on nanoporous templates through selective surface functionalization constitutes an important step toward the ultimate goal of precisely engineered nanomaterials.

Acknowledgment. Work at LLNL was performed under the auspices of the U.S. DOE by LLNL under Contract DE-AC52-07NA27344.

CM900636S

(28) Bolland, J. L. *Proc. R. Soc. London, Ser. A* **1946**, 186, 218.

(29) Hartney, M. A.; Hess, D. W.; Soane, D. S. *J. Vac. Sci. Technol. B* **1989**, 7 (1), 1.

(30) Lehmann, O.; Stuke, M. *Appl. Phys. A: Mater. Sci. Process* **1991**, 53, 343.

(31) George, M. C.; Mqhras, A.; Piech, M.; Bell, N. S.; Lewis, J. A.; Braun, P. V. *Adv. Mater.* **2009**, 21, 66.

(32) Dulcey, C. S.; Georger, J. H.; Chen, M.-S.; McElvany, S. W.; O'Ferrall, C. E.; Benezra, V. I.; Calvert, J. M. *Langmuir* **1996**, 12, 1638.